Published in final edited form as:
Science. 2014 March 14; 343(6176): 1260–1263. doi:10.1126/science.1248943.

Complement Is Activated by IgG Hexamers Assembled at the Cell Surface

Christoph A. Diebolder[1,2,*], **Frank J. Beurskens**[3,*], **Rob N. de Jong**[3], **Roman I. Koning**[2], **Kristin Strumane**[3], **Margaret A. Lindorfer**[4], **Marleen Voorhorst**[3], **Deniz Ugurlar**[1], **Sara Rosati**[5], **Albert J. R. Heck**[5], **Jan G. J. van de Winkel**[3,6], **Ian A. Wilson**[7,8], **Abraham J. Koster**[2], **Ronald P. Taylor**[4], **Erica Ollmann Saphire**[9], **Dennis R. Burton**[8,9,10], **Janine Schuurman**[3], **Piet Gros**[1,†], and **Paul W. H. I. Parren**[3,†]

[1]Crystal and Structural Chemistry, Bijvoet Center for Biomolecular Research, Department of Chemistry, Faculty of Science, Utrecht University, 3584 CH Utrecht, Netherlands [2]Department of Molecular Cell Biology, Electron Microscopy Section, Leiden University Medical Center, 2300 RC Leiden, Netherlands [3]Genmab, 3584 CM Utrecht, Netherlands [4]Department of Biochemistry and Molecular Genetics, University of Virginia School of Medicine, Charlottesville, VA 22908, USA [5]Biomolecular Mass Spectrometry and Proteomics, Bijvoet Center for Biomolecular Research and Utrecht Institute for Pharmaceutical Sciences, Utrecht University, 3584 CH Utrecht, Netherlands [6]Department of Immunology, University Medical Center, 3584 CX Utrecht, Netherlands [7]Department of Integrative Structural and Computational Biology, The Scripps Research Institute, La Jolla, CA 92037, USA [8]IAVI Neutralizing Antibody Center and Center for HIV/AIDS Vaccine Immunology and Immunogen Discovery, The Scripps Research Institute, La Jolla, CA 92037, USA [9]Department of Immunology and Microbial Science, The Scripps Research Institute, La Jolla, CA 92037, USA [10]Ragon Institute of MGH, MIT, and Harvard, Cambridge, MA 02139, USA

Abstract

Complement activation by antibodies bound to pathogens, tumors, and self antigens is a critical feature of natural immune defense, a number of disease processes, and immunotherapies. How antibodies activate the complement cascade, however, is poorly understood. We found that specific noncovalent interactions between Fc segments of immunoglobulin G (IgG) antibodies resulted in the formation of ordered antibody hexamers after antigen binding on cells. These hexamers recruited and activated C1, the first component of complement, thereby triggering the complement cascade. The interactions between neighboring Fc segments could be manipulated to block, reconstitute, and enhance complement activation and killing of target cells, using all four

†Corresponding author: p.parren@genmab.com (P.W.H.I.P.); p.gros@uu.nl (P.G.).
*These authors contributed equally to this work.

Supplementary Materials
www.sciencemag.org/content/343/61XX/page/suppl/DC1
Materials and Methods
Supplementary Text
Figs. S1 to S6
Tables S1 to S3
References (*33–62*)

human IgG isotypes. We offer a general model for understanding antibody-mediated complement activation and the design of antibody therapeutics with enhanced efficacy.

Complement activation by antibodies initiates immune protection through the generation of an array of biologically active products including opsonins, anaphylatoxins, chemotactic agents, and membrane attack complexes (1, 2). The classical pathway of complement is triggered when antigen-bound immunoglobulin M (IgM) or IgG antibody molecules bind C1, which consists of the multimeric pattern recognition molecule C1q and a heterotetramer of the proteases C1r and C1s (3, 4). C1q binds a single IgG Fc segment with very low affinity (dissociation constant $K_d \approx 10^{-4}$ M) (5, 6), and physiological C1 binding thus requires an increase in the apparent binding constant—for instance, through antigen-driven antibody clustering, which allows multivalent C1q binding (7). The molecular events governing complement activation, including the C1-antibody stoichiometry required for optimal activation, remain poorly understood (3, 8–13). Here, we set out to characterize and visualize the first steps in complement activation by IgG at the molecular level.

In the structure of human anti–HIV-1 gp120 antibody IgG1-b12 at 2.7 Å resolution [Protein Data Bank (PDB) entry 1HZH] (14, 15), the IgG Fc segments are arranged in a hexameric ring (Fig. 1A). A similar crystal packing is found for human antibody 2G12 (16). The spatial orientation of Lys^{322} (Fig. 1A), a critical residue in the C1q binding site on IgG, suggested a compatibility of the hexamer with the arrangement of the six antibody-binding headpieces in C1q. We hypothesized that IgG antibodies activate complement-dependent cytotoxicity (CDC) via ordered clustering into hexamers through specific noncovalent Fc interactions. To investigate this hypothesis, we used a peptide that has been shown to bind residues in the observed Fc-Fc interface (17) (Fig. 1B). The peptide inhibited CDC of human B cell lymphomas by CD20 antibody IgG1-7D8 and CD38 antibody IgG1-005 (Fig. 1C), both of which potently induce CDC by the classical pathway (18, 19). Next, we generated interface mutations designed to weaken Fc-Fc interactions. We confirmed that antigen binding and C1q binding to randomly immobilized IgG1 (fig. S1) were mostly unaffected by the mutations. In contrast, the apparent avidity of C1q for cell-bound IgG1-7D8 mutated at positions Ile^{253}, His^{433}, or Asn^{434} decreased by as much as a factor of 20 (Fig. 1D, fig. S2A, and table S1); this resulted in reduced complement activation and CDC, consistent with other mutations in the Fc-Fc interface (Fig. 1E, fig. S2A, and table S2). Modeling suggested that Lys^{439} and Ser^{440} could be manipulated to test Fc-Fc interactions in a gain-of-function experiment (fig. S2B). In isolation, charge repulsion in mutants K439E ($Lys^{439} \rightarrow$ Glu) and S440K ($Ser^{440} \rightarrow$ Lys) indeed inhibited CDC; this inhibition could be overcome with double mutants or mixtures containing both mutants that neutralized this repulsion (Fig. 1, F and G, and tables S1 and S2).

We also identified mutations that resulted in significantly enhanced CDC, as exemplified by E345R ($Glu^{345} \rightarrow$ Arg), which increased C1q avidity to opsonized cells by a factor of ~5 and CDC by a factor of ~10 when introduced into CD20 antibody IgG1-7D8 (Fig. 2A and tables S1 and S2) (20). Similarly, the E345R substitution increased CDC of CD38 antibody IgG1-005 (Fig. 2B) as well as of its IgG2, IgG3, and IgG4 isotype variants (Fig. 2C). A triple mutant, IgG1-005-RGY, combining E345R with two additional enhancing mutations

[E430G ($Glu^{430} \rightarrow Gly$) and S440Y ($Ser^{440} \rightarrow Tyr$)] readily formed hexamers in solution. The presence of monomeric and hexameric species of IgG1-005-RGY, presumably in equilibrium, was demonstrated by native mass spectrometry (Fig. 3A and table S3), high-performance size exclusion chromatography (HP-SEC) combined with multi-angle static light scattering (MALS) (Fig. 3B), and negative-stain electron tomography (ET) (Fig. 3, C to F). Solution-phase hexamers of IgG1-005-RGY directly activated complement when added to human serum, as shown by the generation of C4d (Fig. 2D). This was also observed for IgG1-7D8-RGY, a triple mutant of the CD20 antibody. Together, these findings directly link a biophysically characterized noncovalent IgG1 hexamer with classical pathway complement activation. Finally, IgG1-005-RGY showed a further potency increase when bound to cells, as shown by stronger CDC at low concentrations relative to the single mutant (Fig. 2E), which may be explained by preformed hexamers or enhanced Fc-Fc–mediated assembly on the cell surface.

To image C1 binding to antigen-bound IgG on a membrane, we performed cryo–electron tomography (cryo-ET) using dinitrophenyl (DNP)–labeled liposomes (20). In the cryo-ET reconstructions, antibodies on the liposome surface assembled in single-layer patches with maximum density at a distance of 11 nm from the membrane (fig. S3, A and E) (20). Addition of purified C1- and C4-depleted serum or normal human serum resulted in C1 binding on top of the antibody layer (fig. S3, F to H). Cryo-ET tomograms of 107 particles representing antibody-C1 complexes were averaged (fig. S4), resulting in an electron density map at low (>6 nm) resolution. The map showed a lower platform at 11 nm (coinciding with the maximum density observed on liposomes with antibody alone), a second platform at 20 nm, and a stalk on top of the upper platform (Fig. 4A). Horizontal sections through the tomogram indicated that the lower platform was composed of a continuous disk with six poorly resolved densities protruding toward the membrane and four discernible densities on top, arranged as an incomplete hexagon (Fig. 4, B to E). We generated a model of the C1-antibody complex by docking the 1HZH crystal packing [adapted by Fab rotation (fig. S5)] into the lower platform and manually fitting C1q headpieces (Fig. 4F and fig. S6) (20). The four densities on top of the lower platform suggested incomplete (4:6) C1q headpiece binding to the antibody hexamer (Fig. 4C) and may reflect flexibility and dynamics of the C1q-IgG interactions.

The model suggested that one Fab arm of each antibody in the hexamer bound the membrane-associated antigen while the other Fab arm was positioned at the height of the platform (Fig. 4F). To test the concept that complement activation might only require monovalent binding, we generated functionally monovalent bispecific antibodies (20, 21) that contained one specific and one innocuous Fab arm (i.e., IgG1-7D8/b12 and IgG1-2F8/b12, monovalently binding CD20 and EGFR, respectively). Both antibodies induced efficient CDC of relevant target cells (Fig. 4, G and H), which for the bispecific antibody 2F8/b12 was strongly enhanced relative to the parental 2F8 antibody. Thus, for this antibody-antigen pair, monovalent binding is better able than (high-affinity) bivalent binding to accommodate the Fc-Fc hexamerization required for efficient CDC.

The hexameric IgG-C1 binding model (Fig. 4, A and F, and fig. S6) revealed geometrical restraints that could explain the strong antigen and epitope dependency of complement

activation. Potent complement activation by monoclonal antibodies is restricted to certain antigens and epitopes (12, 19, 22), presumably because antigen size, density, and fluidity may affect activation (18, 22–26) and because IgG orientation resulting from epitope geometry imposes additional structural constraints (12, 19, 22, 25, 27). Polyclonal antibodies appear to be less sensitive than monoclonal antibodies to such constraints (24, 28, 29), potentially because binding of antibodies to a variety of antigens or epitopes facilitates clustering of Fc segments, thereby allowing efficient Fc-Fc assembly. Monovalent binding of IgG molecules in the platform is consistent with earlier observations (30) and could be envisaged to provide more degrees of freedom for the Fc segments, allowing their optimal positioning for C1q recruitment.

Our model is in agreement with an evolutionary relationship between IgM and IgG in triggering complement (11). IgM normally exists in a polymeric state, in which C1q binding sites are sequestered and only become exposed when antigen is bound (6, 31), whereas IgG normally exists in a monomeric state in which C1q binding sites are exposed but affinity is too low to allow adequate C1 binding. In our model, sequential antigen and Fc-Fc binding by IgG leads to the formation of hexamers that bind C1q with high avidity and activate complement. The model is nonetheless compatible with observations that smaller IgG complexes may suffice to initiate some complement activation (8, 32). However, low-avidity C1q binding will result in only modest complement activity (27), whereas the IgG hexamer will bind C1q most avidly, thus ensuring optimal complement activation when required.

The observation that IgG hexamerization after antigen binding leads to effective complement activation could be exploited by increasing Fc-Fc contact formation. Because the E345R mutation bestowed complement-activating capability on all human IgG isotypes, IgG hexamerization may be a general concept applicable to the engineering of therapeutic antibodies with enhanced activity.

Supplementary Material

Refer to Web version on PubMed Central for supplementary material.

Acknowledgments

We thank M. Daha for purified C1, and F. G. A. Faas and W. Vossenaar-Horstman for technical support. Supported in part by European Research Council advanced grant 233229; Cyttron II (LSH framework FES0908); the Netherlands Centre for Electron Nanoscopy (NeCEN), Leiden; the Netherlands Organization for Scientific Research (NWO); and the European Regional Development Fund of the European Commission. D.R.B. is supported by National N Institute of Allergy and Infectious Diseases (NIAID) grant AI055332. I.A.W. is supported by NIAID grant AI084817. The data presented are tabulated in the main paper and in the supplementary materials. The ET data presented are archived at EMDataBank, entries EMD-2506, EMD-2507, and EMD-2554. F.J.B., R.N.d.J., K.S., M.V., J.G.J.v.d.W., J.S., and P.W.H.I.P. are Genmab employees and own Genmab warrants and/or stock. A.L., R.P.T., S.R., and A.J.R.H. received Genmab funding. F.J.B., R.N.d.J., J.S., and P.W.H.I.P. are inventors on Genmab patent applications related to technology to enhance complement activation.

References and Notes

1. Ricklin D, Hajishengallis G, Yang K, Lambris JD. Nat Immunol. 2010; 11:785–797. [PubMed: 20720586]

2. Dunkelberger JR, Song WC. Cell Res. 2010; 20:34–50. [PubMed: 20010915]
3. Gaboriaud C, et al. Trends Immunol. 2004; 25:368–373. [PubMed: 15207504]
4. Kishore U, Reid KB. Immunopharmacology. 2000; 49:159–170. [PubMed: 10904115]
5. Hughes-Jones NC, Gardner B. Mol Immunol. 1979; 16:697–701. [PubMed: 119162]
6. Feinstein A, Richardson N, Taussig MJ. Immunol Today. 1986; 7:169–174. [PubMed: 25290202]
7. Burton DR. Mol Immunol. 1985; 22:161–206. [PubMed: 3889592]
8. Borsos T, Rapp HJ. Science. 1965; 150:505–506. [PubMed: 5319759]
9. Rosse WF. J Clin Invest. 1971; 50:727–733. [PubMed: 4995527]
10. Thompson JJ, Hoffman LG. Immunochemistry. 1974; 11:537–541. [PubMed: 4459262]
11. Burton DR. Immunol Today. 1986; 7:165–167. [PubMed: 25290200]
12. Bindon CI, Hale G, Waldmann H. Eur J Immunol. 1988; 18:1507–1514. [PubMed: 2973413]
13. Burton DR. Trends Biochem Sci. 1990; 15:64–69. [PubMed: 2186517]
14. Saphire EO, Parren PWHI, Barbas CF 3rd, Burton DR, Wilson IA. Acta Crystallogr D. 2001; 57:168–171. [PubMed: 11134947]
15. Saphire EO, et al. Science. 2001; 293:1155–1159. [PubMed: 11498595]
16. Wu Y, et al. Cell Rep. 2013; 5:1443–1455. [PubMed: 24316082]
17. DeLano WL, Ultsch MH, de Vos AM, Wells JA. Science. 2000; 287:1279–1283. [PubMed: 10678837]
18. Teeling JL, et al. Blood. 2004; 104:1793–1800. [PubMed: 15172969]
19. de Weers M, et al. J Immunol. 2011; 186:1840–1848. [PubMed: 21187443]
20. See supplementary materials on *Science* Online.
21. Labrijn AF, et al. Proc Natl Acad Sci USA. 2013; 110:5145–5150. [PubMed: 23479652]
22. Cragg MS, et al. Blood. 2003; 101:1045–1052. [PubMed: 12393541]
23. Parce JW, Kelley D, Heinzelmann K. Biochim Biophys Acta. 1983; 736:92–98. [PubMed: 6606439]
24. Hughes-Jones NC, Gorick BD, Howard JC, Feinstein A. Eur J Immunol. 1985; 15:976–980. [PubMed: 2996908]
25. Teeling JL, et al. J Immunol. 2006; 177:362–371. [PubMed: 16785532]
26. Xia MQ, Hale G, Waldmann H. Mol Immunol. 1993; 30:1089–1096. [PubMed: 8366859]
27. Pawluczkowycz AW, et al. J Immunol. 2009; 183:749–758. [PubMed: 19535640]
28. Dechant M, et al. Cancer Res. 2008; 68:4998–5003. [PubMed: 18593896]
29. Kushihata F, Watanabe J, Mulder A, Claas F, Scornik JC. Transplantation. 2004; 78:995–1001. [PubMed: 15480164]
30. Watts HF, Anderson VA, Cole VM, Stevenson GT. Mol Immunol. 1985; 22:803–810. [PubMed: 3849671]
31. Czajkowsky DM, Shao Z. Proc Natl Acad Sci USA. 2009; 106:14960–14965. [PubMed: 19706439]
32. Rosse WF, Rapp HJ, Borsos T. J Immunol. 1967; 98:1190–1195. [PubMed: 6026745]

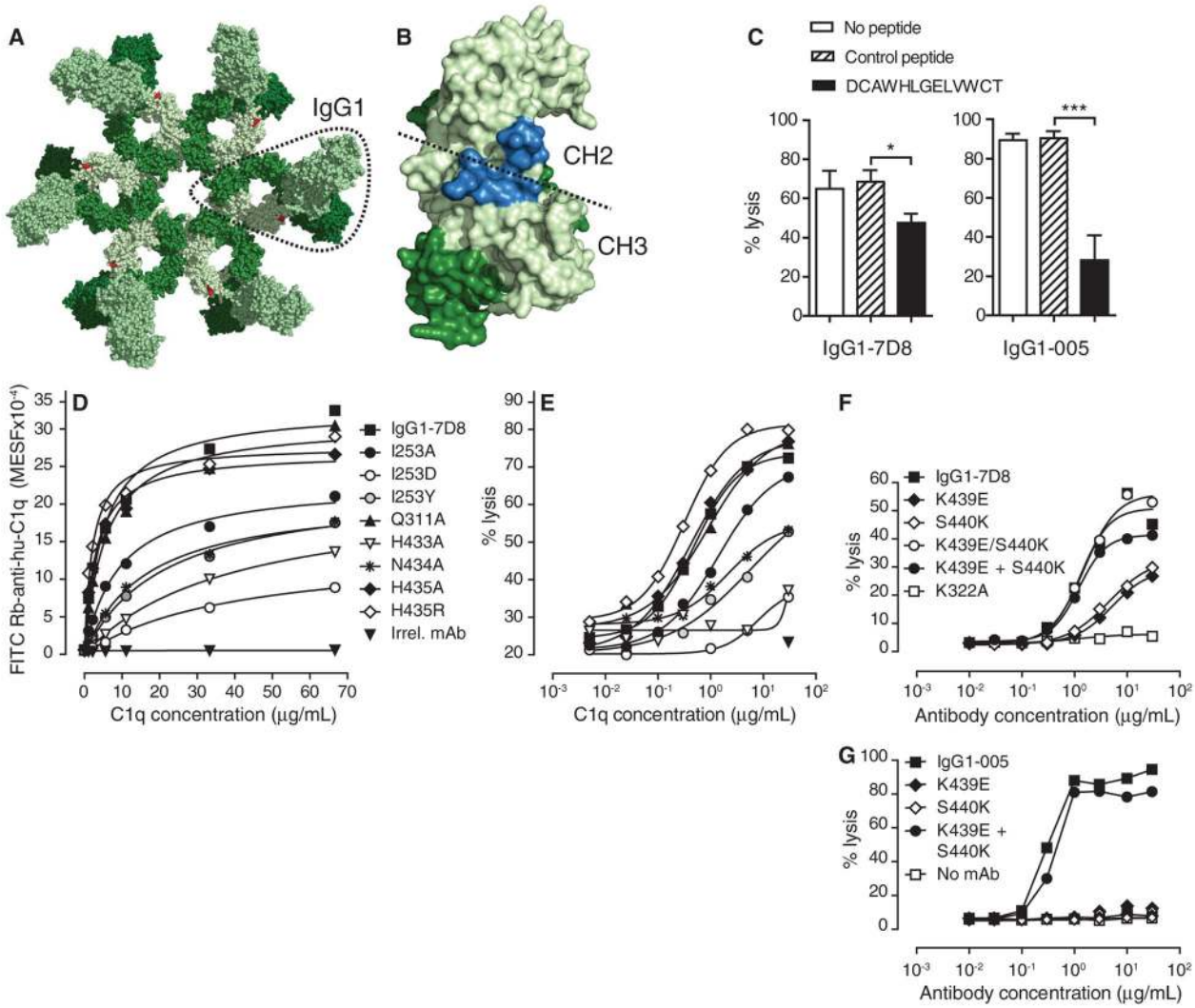

Fig. 1. C1q binding and complement activation by antibody hexamers

(**A**) IgG hexamer crystal packing of IgG1-b12 (1HZH). The dashed enclosure indicates a single IgG molecule. The C1q binding residue Lys^{322} is indicated in red. (**B**) Surface map depicting the Fc-Fc interface. Residues interacting with the Fc-binding peptide DCAWHLGELVWCT are indicated in blue. (**C**) The Fc-binding peptide inhibits CDC mediated by IgG1-7D8 (Raji cells) and IgG1-005 (Daudi cells). Data are average values ± SD ($N = 3$); one-way analysis of variance followed by Dunnett's multiple comparison post hoc test: $^{*}P < 0.05$, $^{***}P < 0.001$. (**D**) C1q binding to $CD20^{+}$ Raji cells opsonized with wild-type or mutated CD20 antibody IgG1-7D8. MESF, molecules of equivalent soluble fluorochrome. A representative example is shown ($N = 3$). (**E**) CDC of Raji cells opsonized with wild-type and mutated IgG1-7D8. A representative example is shown ($N = 3$). The absence of CDC without added C1q indicates classical pathway activation. (**F** and **G**) CDC of K439E and S440K, abrogated in single point mutants, is restored in an IgG1-7D8 double mutant [(F), Raji cells] and by mixing single mutants of IgG1-7D8 (F) or IgG1-005 [(G), Daudi cells]. Representative examples are shown ($N = 3$). Amino acid abbreviations: A, Ala;

C, Cys; D, Asp; E, Glu; F, Phe; G, Gly; H, His; I, Ile; K, Lys; L, Leu; M, Met; N, Asn; P, Pro; Q, Gln; R, Arg; S, Ser; T, Thr; V, Val; W, Trp; Y, Tyr.

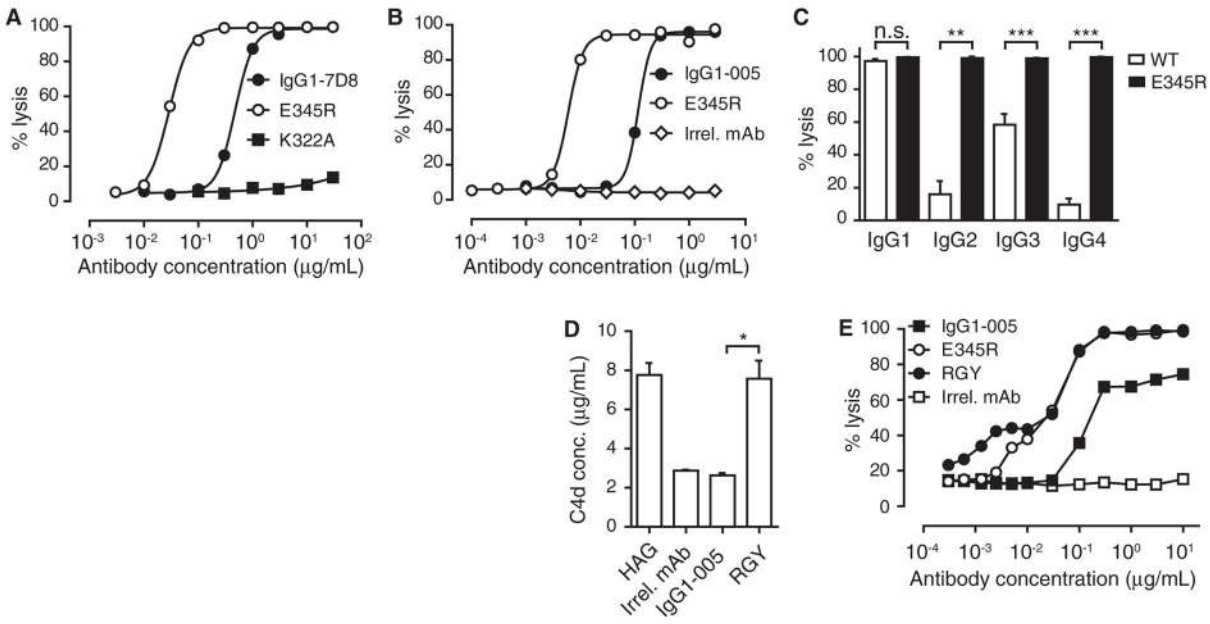

Fig. 2. Increased CDC by enhanced hexamer formation

(**A** and **B**) Increased CDC of Daudi cells by IgG1-7D8-E345R (A) and IgG1-005-E345R (B) relative to wild-type antibodies. Representative examples are shown ($N = 4$). (**C**) E345R mutants of IgG1-005 isotype variants induces CDC of Daudi cells more potently than wild-type (WT) IgG2, IgG3, and IgG4; IgGs were tested at 10 μg/ml. Data are average values ± SD ($N = 3$); two-sided unpaired t test with Welch's correction: n.s., not significant; $^{**}P < 0.01$, $^{***}P < 0.001$. (**D**) IgG1-005-RGY induced C4d generation in normal human serum. Data are average values ± SD ($N = 3$). Two-sided unpaired t test with Welch's correction; $^{*}P < 0.05$. Heat-aggregated IgG (HAG) was used as a positive control. (**E**) IgG1-005-RGY showed enhanced CDC activity of Ramos cells relative to wild-type IgG1-005 and IgG1-005-E345R. A representative example is shown ($N = 3$).

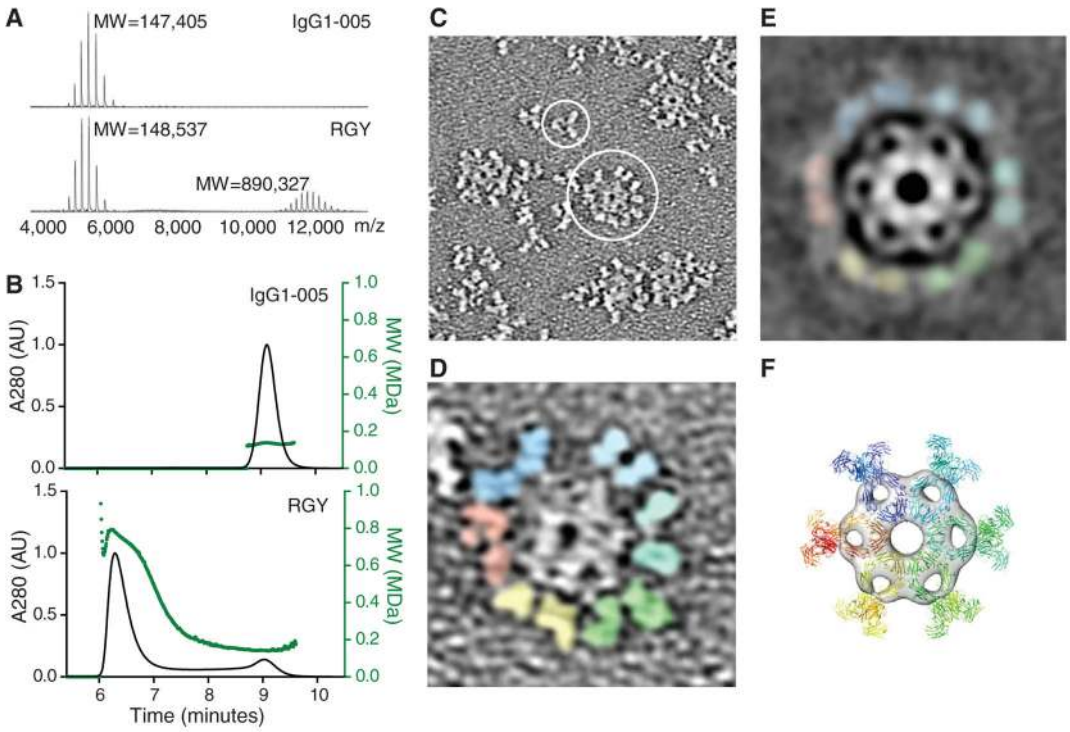

Fig. 3. Solution-phase hexamers formed by triple mutant IgG1-005-RGY

(**A**) Native mass spectrometry of IgG1-005 indicating a molecular weight (MW) of 147,405 daltons and IgG1-005-RGY showing MWs of a monomer (148,537 daltons) and a hexamer (890,327 daltons) (table S3). The hexameric state was confirmed in experiments using different conditions ($N = 6$); *m/z*, mass/charge ratio. (**B**) Overlay of HP-SEC–MALS profiles [absorbance at 280 nm (A280), black, left axis; MW, green, right axis] of IgG1-005 (top) and IgG1-005-RGY (bottom) shows that ~79% IgG1-005-RGY eluted as hexamer and ~21% as monomer, whereas >99% of IgG1-005 eluted as monomer. A representative example is shown ($N = 3$). (**C** to **F**) ET of negatively stained IgG1-005-RGY. (C) ET overview image showing a monomer (small circle) and a hexamer (large circle). (D) Representative hexamer with colored Fab pairs. (E) ET average of 200 subtomograms at a resolution of 2.9 nm. (F) Surface rendering of a symmetrized Fc ring with docked 1HZH hexamer.

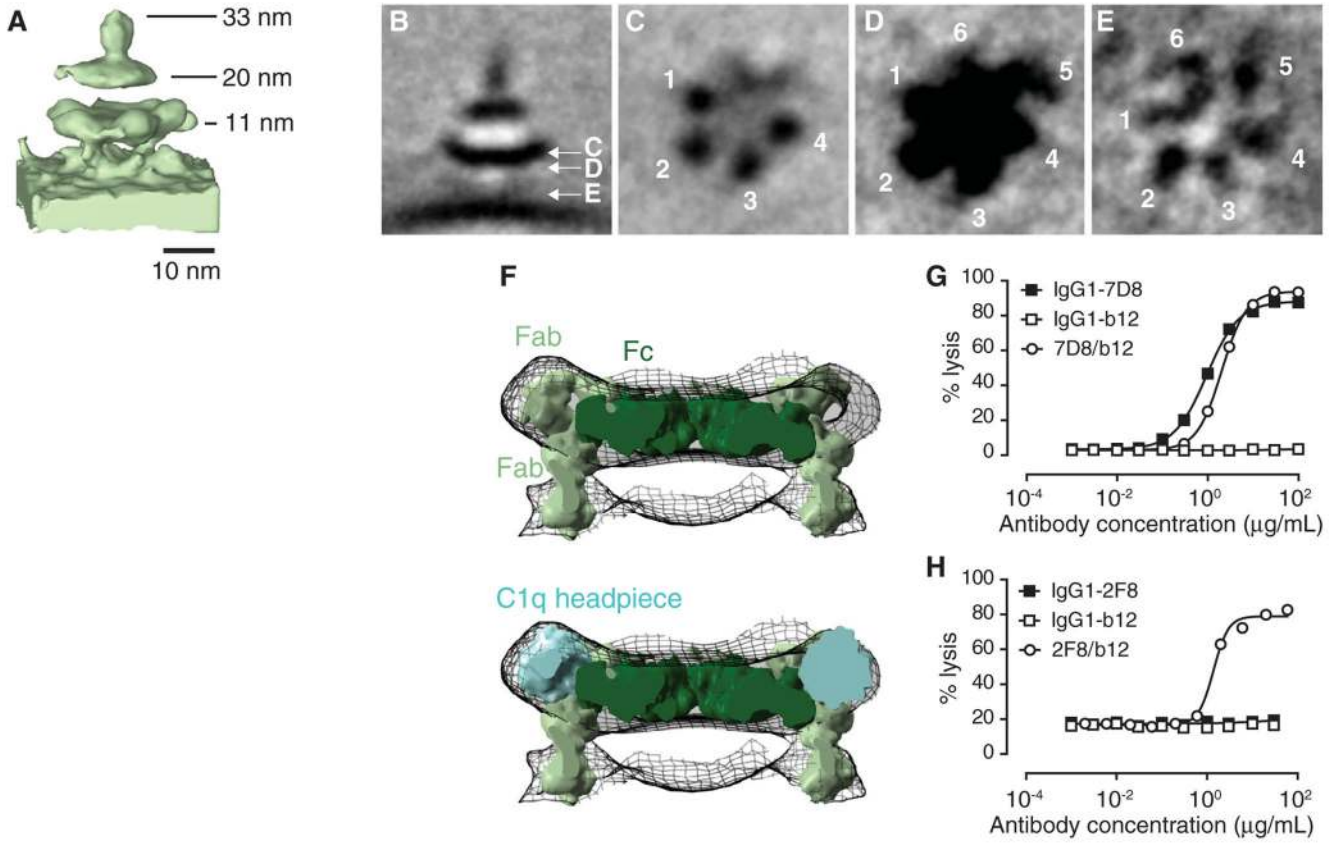

Fig. 4. Visualization of antibody-C1 complexes on antigen-coated liposomes

(**A**) Subtomogram average of antibody-C1 at >6 nm resolution shown as an isosurface. Heights indicate distances to the membrane center. (**B**) Vertical section through cryo-ET average. White arrows indicate the positions of sections shown in (C) to (E). (**C**) Top horizontal section showing four putative C1q globular headpieces. (**D**) Center section showing a dense hexagonal platform. (**E**) Bottom section showing six putative antigen-binding Fab arms. (**F**) Side view of the IgG1-b12–based hexamer model placed into the six-fold symmetrized density of the lower cryo-ET platform (top) and hexamer model with docked C1q headpieces (bottom). (**G**) CDC of $CD20^+$ Raji cells by (functionally monovalent) bispecific antibody IgG1-7D8/b12. A representative example is shown ($N = 3$). (**H**) CDC of $EGFR^+$ A431 cells by (functionally monovalent) bispecific antibody IgG1-2F8/b12. A representative example is shown ($N = 4$). IgG1-b12 against HIV-1 gp120 contributed the innocuous Fab arm.